AIAA 2017-0808
AIAA SciTech Forum
9 - 13 January 2017, Grapevine, Texas
AIAA Modeling and Simulation Technologies Conference

Sensitivity of Unmanned Aerial Vehicle Model-Aided Navigation

Stéphane D'Urso* and Jason Gross†
West Virginia University, Morgantown, WV, 26506, USA

To overcome the rapid and unbounded error growth of low-cost Inertial Navigation Systems (INS), aircraft localization methods commonly compensate for Inertial Measurement Unit (IMU) sensor errors by integrating them with Global Positioning System (GPS) measurements via a Kalman Filter. However, over the past decade, the potential of GPS jamming or even spoofing GPS signals has focused the research community on the development of GPS-denied navigation technologies. Of the GPS-denied techniques, one approach that has been considered is the use of a Vehicle Dynamic Models (VDM) to reduce the rate at which an INS becomes unusable. As such, this paper considers the use of an aerodynamic model to aid in compensation of IMU errors of a fixed-wing Unmanned Aerial Vehicle (UAV). The goals of this paper are to evaluate the sensitivity of the performance of dynamic model aided navigation in the context of low-cost platforms where performance benefit must be weighed against the complexity that is required to develop the dynamic model. To do this, first, the sensitivity to the required modeling accuracy is shown by perturbing the the model coefficients with errors. In addition, different sensors and sensor grades are evaluated, and three different model-aided navigation architectures are discussed and evaluated. To conduct this work, a UAV simulation is developed within which a UAV trajectory is driven by 'truth' dynamic model and then IMU measurements are derived and errors are added to them using standard stochastic models for IMU sensors. In preparation for UAV flight tests, this performance sensitivity study is conducted to characterize the expected performance.

I. Introduction

Multiple authors have considered model-aided navigation. For example, Koifman, M. and Bar-Itzhack introduced an approach in which the model of aircraft dynamics, mathematically modeled is coupled with conventional INS system within an Extended Kalman Filter (EFK) to obtain a navigation system with performances considerably better than simply allowing the INS to drift.[1] In this study, it is demonstrated that the dynamics aided INS is more accurate than the unaided INS and, at the same time, that this aided navigation technique allows better calibration of its own error sources if combined with a GPS system. Further, Crocoll et al.[2] introduced an Unified Model (UM) that implicitly constrains the two independent state prediction models (i.e. VDM and INS) to reduce computation burden and state vector when implementing model-aided navigation. Crocoll et. al[3] then used the same UM technique for an experimental quadcopter application in which they demonstrated that even though no rotational vehicle dynamics are modeled (they use only translational dynamics modeling), roll angles, pitch angles and even IMU biases with bounded errors are estimable with model-aided navigation. For fixed-wing aircraft, Bryson and Sukkarieh,[4] considered using a Vehicle Dynamic Models (VDM) to predict the aircraft state vector which are then fused with the IMU measurements via an EKF to estimate the errors in the inertial sensors and in the VDM computations. In this work, they showed that the simulation results related to the different INS configurations considered improves the navigation system performance even when small parameter errors are present in the model. Further, it is shown that IMU bias estimation depends mainly on sudden acceleration errors in the VDM and also on growing errors in the VDM velocity and Euler angles. More recently, Khagani and Skaloud[5]

*Graduate Research Assistant, Department of Mechanical and Aerospace Engineering (MAE), Morgantown, WV , AIAA Student Member

†Assistant Professor, Department of MAE, Morgantown, WV , AIAA Senior Member

used a conventional INS/GNSS setup to be used for small UAVs with low-cost IMUs. In their work, they provide a VDM that estimates of position, velocity, and attitude, which is updated within a filter based on available; they also consider GNSS outages and discuss about observability.

Because of these promising results, this paper motivation is provide additional insight as to the sensitivity of the required quality of the UAV dynamic model, IMU sensor grade, and effects of additional sensors. The rest of this paper is organized as follows. Section II discusses at high-level the UAV dynamic model approach considered, the UAV that this study is based upon, and the simulation environment developed for this study. Next, Section III details the aircraft equations of motions and force and moment equations as well as the specific INS mechanization adopted in the study. Section IV shows all the results obtained considering all the case studies investigated. Finally, the conclusions and some future developments suggestions are discussed in Section V.

II. Technical Approach

In order to achieve the overall objective, a numerical method was used to create the aerodynamic model of the aircraft. This model provides the coefficients and parameters that have to be used in the VDM. The model is derived based on the Vortex Lattice Method (VLM), which represents the lifting surfaces and their trailing wakes as single -layer vortex sheets, discretized into horseshoe vortex filaments, whose trailing legs are assumed to be parallel to the UAV body x-axis. VLM results are known to be high fidelity, offering detailed information, such as surface loading.[6]

II.A. Dynamic Modeling

The small UAV modeled in this work is the West Virginia University Phastball Zero (PZero) UAV, which has a wing span of 2.4 m and a weight of 12.5 kg. The first step for the development of each model was to define the operating points and the reference Reynolds numbers as shown in Figure 4(a) knowing the PZero UAV speed and airfoil geometry. Subsequently, each lifting surface were paneled, as shown in Figure 4(b), in order to use the VLM to estimate the pressure distribution as shown in Figure 4(c) and the stability derivatives to be used to solve the equations of motion for the VDM. The fuselage and the engines have been also considered in the VLM modeling in order to use a model as accurate as possible unlike of the other additional ancillary components, which are modeled in our CAD rendering (e.g., landing gears and antennas).

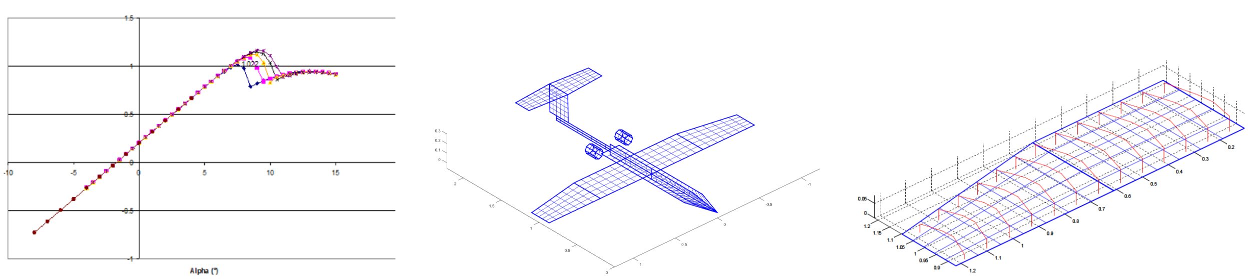

(a) Reynolds number behavior for wing profile

(b) VLM paneling

(c) Pressure distribution

Figure 1: Aerodynamic analysis through VLM

The mass and moments of inertia were estimated using 3D CAD software (CATIA V5). Except for wires and cabling, all the parts have been drawn in order to obtain a detailed mass distribution.

II.B. Flight Simulation and Sensor Error Models

For trajectory generation, a six degree-of-freedom (6DoF), Simulink[7] model has been created. The approach allows the user to run the Simulink model of the aircraft, and simultaneously animate it in the free, open source multi-platform flight simulator FlightGear,[8] as shown in Figure 2(b). Pilot commands are managed through a joystick or through an input script file. In this study, five constant-height flights, each 5 minutes

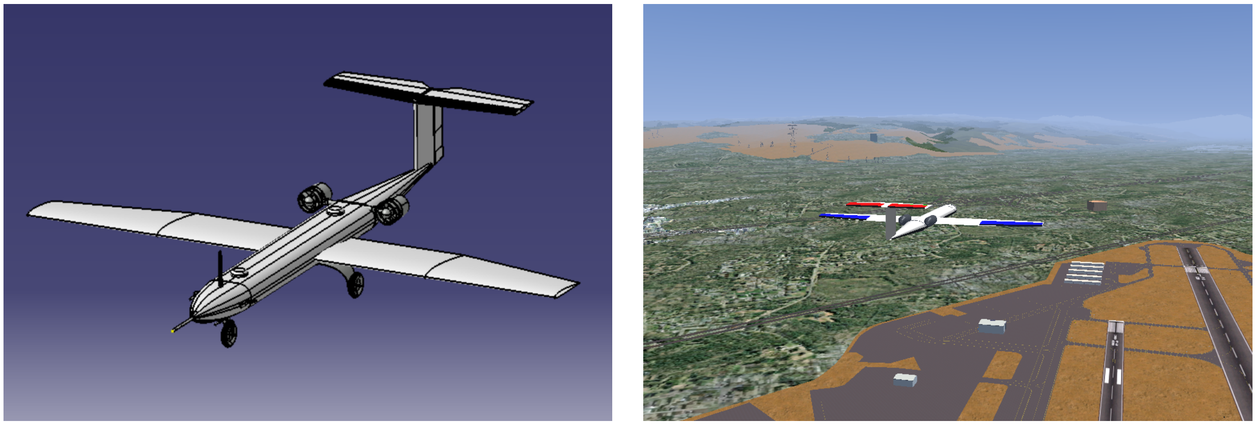

(a) CAD model

(b) Flight simulator interface (FlightGear)

Figure 2: Geometrical model

in length characterized by little variations of the deflection angles relative to the elevator and aileron were simulated.

Using the output of the simulated flight trajectory, IMU sensors are then derived using a Inertial Navigation System Matlab toolbox[9] which has been modified to model various grade IMUs.[10] The reference IMU device is a tactical grade Honeywell HG1930BA50 which characteristics are shown in the Table 1, and one IMU much worse than these (i.e., automotive grade) and one IMU much better than this (i.e., intermediate grade) were also considered.

Table 1: Honeywell HG1930BA50 Performance[11]

Gyro Bias Repeatability	40 °/h 1σ
Gyro Bias In-run Stability	1.5 kg
Angular Random Walk (ARW)	0.09^5, 0.09^5 °/$\sqrt{\text{h}}$ max
Accel Bias Repeatability	10 mg 1σ
Accel Bias In-run Stability	0.5 kg 1σ
Velocity Random Walk (VRW)	0.3 fps/$\sqrt{\text{h}}$ max

III. Model-Aided Navigation Architecture

The architecture of the algorithm used in this work consists of two subsystems: the first is related to the INS that estimates position, velocity and attitude of the aircraft using the IMU data while the second the VDM which also estimates velocity and attitude through the equation of motion and estimated forces and movements based on the coefficients from VLM.

III.A. Vehicle Dynamic Model

For the VDM section, in order to estimate velocity and attitude, the following equations of motion that assumed flat Earth were used:[12]

$$\dot{u} = rv - qw + gx + (F_x/m) \tag{1}$$

$$\dot{v} = pw - ru + gy + (F_y/m) \tag{2}$$

$$\dot{w} = qu - pv + gz + (F_z/m) \tag{3}$$

$$\dot{p} = \frac{\{I_{zz}\ l + I_{xz}\ N - [I_{xz}\ (I_{yy} - I_{xx} - I_{zz})]\ pq + [I_{xz}^2 + I_{zz}\ (I_{zz} - I_{yy})]rq\}}{(I_{xx}\ I_{zz} - I_{xz}^2)} \tag{4}$$

$$\dot{q} = \frac{1}{I_{yy}}\ [M - (I_{xx} - I_{zz})\ pr - I_{xz}\ (p^2 - r^2)] \tag{5}$$

$$\dot{r} = \frac{\{I_{xz}\ l + I_{xx}\ N - [I_{xz}\ (I_{yy} - I_{xx} - I_{zz})]\ rq + [I_{xz}^2 + I_{xx}\ (I_{xx} - I_{yy})]rq\}}{(I_{xx}\ I_{zz} - I_{xz}^2)} \tag{6}$$

$$\dot{\phi} = p + (q \sin\phi + r\cos\phi)\tan\theta \tag{7}$$

$$\dot{\theta} = q\cos\phi - r\sin\phi \tag{8}$$

$$\dot{\psi} = (q\sin\phi + r\cos\phi)\sec\theta \tag{9}$$

where the gravitational acceleration g_n is defined as

$$g_n = \begin{bmatrix} g_x \\ g_y \\ g_z \end{bmatrix} = \begin{bmatrix} -g\sin\theta \\ g\sin\phi\cos\theta \\ g\sin\phi\cos\theta \end{bmatrix}. \tag{10}$$

The force and moments are expressed by,

$$F_x = C_X \bar{q} S + T_x \tag{11}$$
$$F_y = C_Y \bar{q} S + T_y \tag{12}$$
$$F_z = C_Z \bar{q} S + T_z \tag{13}$$
$$l = C_l \bar{q} S b + M_{T_x} \tag{14}$$
$$M = C_M \bar{q} S c + M_{T_y} \tag{15}$$
$$N = C_N \bar{q} S b + M_{T_z} \tag{16}$$

where $\bar{q} = (1/2)\rho V^2$ is the dynamic pressure, ρ is the atmospheric density, S is the wing surface and T, M_T are the thrusting effects.

The force and moment coefficients have been calculated in the form

$$C_{(\ )} = C_{(\ )}\left(\bar{c}, e_0, b, Æ, \alpha, \beta, V, u, \delta, \dot{\alpha}, p, q, r\right). \tag{17}$$

In the previous equations, $\bar{c}$ is the wing chord, α is the angle of attack, β is the sideslip angle, e_0 is the Oswald efficiency number, $Æ$ is the aspect ratio, b is the wing span, V is the total velocity, u is the forward speed, δ is referred to the aileron, elevator and rudder deflections, $\dot{\alpha}$ is the aerodynamic-angle rate, and p,q and r are the components of the aircraft body-axis angular-velocity vector.

III.B. Inertial Navigation System

For the INS, the mechanization derived in Groves (2013)[13] for positioning in a Earth frame with NED velocity and attitude. In order to calculate position (p_n), velocity (v_n) and Euler angles (Φ) in the North-East-Down (NED) frame n, the following equations are used,

$$\dot{p} = v_n \tag{18}$$

$$\dot{v} = C_b^n f_b + g_n - (\Omega_{en}^n + 2\Omega_{ie}^n)v_n \tag{19}$$

$$\dot{\Phi} = E_b^n w_b \tag{20}$$

where C_b^n is the body to navigation frame transformation matrix, f_b is the body-axis specific force vector, E_b^n is the rotation rate transformation matrix, and w_b is the body-axis angular rate vector.

The third term of Equation (19) takes into account of the Earth's rotation considering the following terms.

$$\Omega_{en}^n = \begin{bmatrix} 0 & -\omega_{en,z}^n & \omega_{en,y}^n \\ \omega_{en,z}^n & 0 & -\omega_{en,x}^n \\ -\omega_{en,y}^n & \omega_{en,x}^n & 0 \end{bmatrix} \tag{21}$$

$$\omega_{en}^n = \begin{bmatrix} v_{eb,E}^n/(R_E(L_b)+h_b) \\ -v_{eb,N}^n/(R_N(L_b)+h_b) \\ (-v_{eb,E}^n \tan L_b)/(R_E(L_b)+h_b) \end{bmatrix} \tag{22}$$

$$\Omega_{ie}^n = \omega_{ie} \begin{bmatrix} 0 & \sin L_b & 0 \\ -\sin L_b & 0 & -\cos L_b \\ 0 & \cos L_b & 0 \end{bmatrix} \tag{23}$$

Furthermore, knowing that $\omega_{ie} = 7.292\,115\,0\,\mathrm{rad/s}^{-1}$ is the WGS 84 Earth's angular rate and,

$$R_N(L_b) = \frac{R_0(1-e^2)}{(1-e^2\sin^2 L_b)^{3/2}} \tag{24}$$

$$R_E(L_b) = \frac{R_0}{\sqrt{(1-e^2\sin^2 L_b)}} \tag{25}$$

where R_N is the radius of curvature for North-South motion, R_E is the radius of curvature for East-West motion, $R_0 = 6\,378\,137\,\mathrm{m}$ is the equatorial radius, $e = 0.0818191918425$ is the eccentricity, and L_b is the geodetic latitude.

III.C. Filter Design

Figure 3 illustrate the configuration used in the proposed approach.

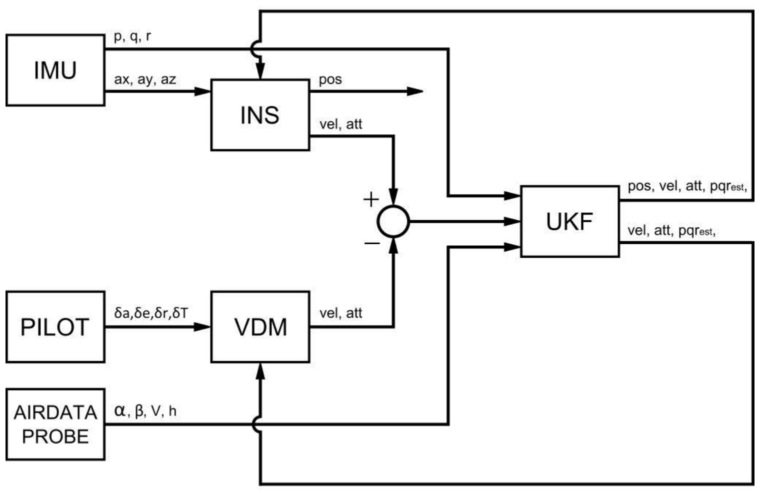

Figure 3: Model Aided Navigation configuration.

As shown in Figure 3, an Unscented Kalman filter (UKF)[14] is used to fuse the outputs from INS and the VDM. For details on how to implement the UKF algorithm, the reader is turned to,[15] in this section, the key elements of of the UKF used in this work including the state vector, $\mathbf{x}$, nonlinear prediction model, f, measurement update model, h, and assumed process noise, Q and measurement noise, R, are outlined .

The state vector $\mathbf{x}$ consists of the following 12 states (position, velocity, body-to-NED Euler angles, and estimated angular rates $[p, q, r]$):

$$\mathbf{x} = [\, x \;\; y \;\; z \;\; V_N \;\; V_E \;\; V_D \;\; \phi \;\; \theta \;\; \psi \;\; p \;\; q \;\; r \,]$$

At each time step,k, the unscented transformation is used to generate a set go sigma-points using the previous epoch, $k-1$, estimated state and error-covariance. Then, state estimates are propagated in time using the INS formulation described in Section III.B, denoted as f.

$$x_k = f(x_{k-1}, e_{k-1}, p_{k-1}) + w_{k-1} \tag{26}$$

It should be noted since the aircraft body-axis rates are included as an estimated states, that these estimated p, q and r are used within the INS mechanism for attitude prediction as opposed to the IMU measured values. Furthermore, these states are predicted as a random-walk process by adding process noise. Next, for the measurement update, h, the same set of sigma points that are used for predicting with INS are within the aircraft vehicle dynamic model (VDM) as described in Section III.A are differenced with the INS predictions to form pseudo-measurements.

$$y_k = h(x_k, e_k, p_k) + v_k \tag{27}$$

In particular, the attitude and velocity predicted with INS within Eq. 26 and the attitude and velocity predicted with VDM are differenced within Eq. 27, such that, with an ideal INS and ideal VDM a pseudo-measurement can be used to take advantage of the information that these difference should be 0. These 6 pseudo-measurements are combined with the IMU measured angular rates p, q and r, such that there are 9 measurements in the baseline model added navigation configuration.

$$z_k = \begin{bmatrix} 0_{1x6} & p_{IMU} & q_{IMU} & r_{IMU} \end{bmatrix} \tag{28}$$

Where the 6 zeros account for the pseudo-measurement constraints, and the angular rate states are directly observed by the IMU,

In addition to these nine baseline measurements, the addition of a three airspeed sensor and one altimeter were also considered as additional configurations. The airspeed and altimeter measurement update equations included within h, when utilized are shown in Equation (29) to (32),

$$u_{\mathrm{m}} = V\cos(\alpha)\cos(\beta) \tag{29}$$

$$v_{\mathrm{m}} = V\sin(\beta) \tag{30}$$

$$w_{\mathrm{m}} = V\sin(\alpha)\cos(\beta) \tag{31}$$

$$a_{\mathrm{m}} = h + \eta \tag{32}$$

where V is the measured airspeed, h is the measured altitude and η is the altimeter measurement noise. In (27), $\hat{X}_k$ is the updated state at time step k, $\hat{x}_{k|k-1}$ is the predicted state at time step k from (26), and $\hat{y}_{k|k-1}$ is the predicted output at time step k from (26).

The 12×12 process noise covariance matrix Q and the 9×9 to 13×13 (depending on the architecture chosen) measurement noise covariance matrix R values are expressed in Table 2.

Table 2: Process noise covariance matrix Q and measurement noise covariance matrix R values.

Process noise covariance matrix Q	Position	5.6×10^{-8} rad
	Velocity	8×10^{-4} m/s
	Attitude	3.05×10^{-8} rad
	Angular Rates	3.05×10^{-6} rad/s
Measurement noise covariance matrix R	Velocity	1 m/s
	Attitude	1 rad
	Angular Rates	1 rad/s
	Airspeed	2 m/s
	Altimeter	1 m

These values were selected based on empirical tuning.

IV. Results

To assess performance sensitivity, the aircraft localization results are computed with the following conditions varied:

- Model-aided navigation architecture(i.e., inclusion of airspeed and altimeter measurements);
- IMU sensor grade (i.e., ranging from automotive to tactical grade);
- UAV dynamic model quality with respect to truth (i.e., perturbing the modeled coefficients with errors).

All results are expressed in terms of velocity and altitude drift for the INS along and integrated navigation approach.

IV.A. Model-aided navigation architecture

First, the three different architectures were considered, depending on the measurement technique adopted as mentioned above, namely:

- VDM-aiding only
- VDM with airspeed measurements
- VDM, with airspeed and altimeter measurements

As shown in Table 3, introducing the airspeed sensor we obtain better results in terms of position, velocity and attitude. The introduction of the altimeter further improves the positioning performance.

Table 3: Model-Aided Navigation architectures results

			Position (m)	Velocity (m/s)	Attitude (deg)
Flight #1		INS	2857.34	26.26	1.28
	VDM only	MAN	3812.93	10.73	0.78
	VDM + Airsp	MAN	2221.26	0.26	0.73
	VDM + Airsp + Alt	MAN	2201.64	0.26	0.74
Flight #2		INS	1964.83	26.26	1.28
	VDM only	MAN	3503.28	10.62	0.83
	VDM + Airsp	MAN	3503.28	10.62	0.83
	VDM + Airsp + Alt	MAN	1637.57	0.25	0.75
Flight #3		INS	5761.41	25.85	1.21
	VDM only	MAN	2786.2	12.12	0.89
	VDM + Airsp	MAN	2823.94	0.25	0.72
	VDM + Airsp + Alt	MAN	2704.73	0.25	0.72
Flight #4		INS	5534.09	25.82	1.22
	VDM only	MAN	4489.31	11.25	0.82
	VDM + Airsp	MAN	3728	0.26	0.72
	VDM + Airsp + Alt	MAN	3709.81	0.26	0.73
Flight #5		INS	5604.81	25.79	1.24
	VDM only	MAN	2919.03	11.8	0.84
	VDM + Airsp	MAN	2755.16	0.26	0.71
	VDM + Airsp + Alt	MAN	2650.9	0.26	0.71

As an example, Figure 4 shows an example of the results obtained for a single case. It is important to note that in all the three architectures, in most respects, the MAN approach results to perform better than the INS alone. That is, velocity and attitude are always better, and overall positioning is typically better.

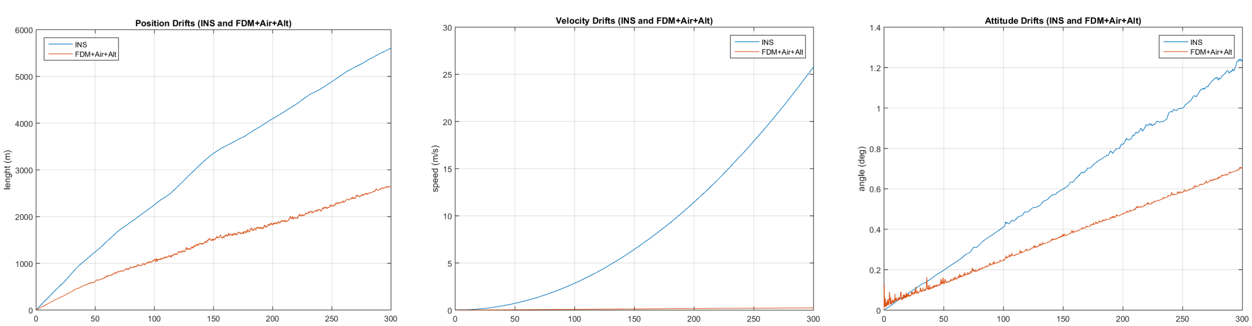

Figure 4: Position,velocity and attitude drifts related to the VDM

IV.B. IMU sensor grade

Next, in order to assess the sensitivity to IMU grade, different scaled versions of the reference IMU listed in Table 1 on page 3, have been created in order to simulate various sensor grades. The results are contained in the Table 4 on the next page.

Table 4: IMU sensor grades' results

			Position (m)	Velocity (m/s)	Attitude (deg)
Flight #1	IMU #1	INS	6110.55	56.59	1.66
		MAN	2046.08	0.18	0.51
	IMU #2	INS	2765.61	25.98	1.27
		MAN	2222.51	0.26	0.74
	IMU #3	INS	2857.34	26.26	1.28
		MAN	2201.64	0.26	0.74
Flight #2	IMU #1	INS	4691.24	63.5	1.41
		MAN	1704.47	0.18	0.8
	IMU #2	INS	2017.02	25.42	1.27
		MAN	1605.4	0.26	0.76
	IMU #3	INS	1964.83	26.26	1.28
		MAN	1637.57	0.25	0.75
Flight #3	IMU #1	INS	9159.58	134.04	4.12
		MAN	68576.87	0.45	1.37
	IMU #2	INS	5785.67	25.8	1.21
		MAN	2706.4	0.25	0.71
	IMU #3	INS	5761.41	25.85	1.21
		MAN	2704.73	0.25	0.72
Flight #4	IMU #1	INS	7096.55	54.53	1.91
		MAN	3729.55	0.27	0.75
	IMU #2	INS	5536.89	25.66	1.22
		MAN	3741.62	0.27	0.74
	IMU #3	INS	5533.96	25.82	1.22
		MAN	3709.81	0.26	0.73
Flight #5	IMU #1	INS	6253.95	28.03	2.48
		MAN	52791.34	0.74	2.19
	IMU #2	INS	5436.11	26.63	1.27
		MAN	2664.19	0.27	0.73
	IMU #3	INS	5604.69	25.8	1.24
		MAN	2650.9	0.26	0.71

As indicated, as expected, the performance typically increases in terms of position and attitude estimation using a better IMU above all switching from IMU#1 scaling factor of 50 times worse than IMU#2, which represents an automotive grade IMU to IMU#2 (Baseline tactical grade IMU), to IMU#3 which has a scaling factor of 1/1000 with respect to IMU#2, which is representative of an intermediate grade IMU. However, this trend is not a severe for MAN approaches. That is, the performance remains fairly consistent for positioning, even as the IMU degrades.

IV.C. UAV dynamic model quality with respect to truth

Finally, the sensitivity to the quality of the aerodynamic model was also investigated by perturbing the value of the model coefficients with 10% and 20% error, respectively.

Within Table 5 the attitude estimate that appears to not be influenced by these variations, however, the position difference gets worse with deteriorating aerodynamic model. However, even at the worst evaluated condition of 20% modeling errors, the integrated navigation is still better than the INS-along. As an example, these results are shown for a single fight, within Figure 5.

Table 5: IMU sensor grades' results

			Position (m)	Velocity (m/s)	Attitude (deg)
Flight #1		INS	2857.34	26.26	1.28
	truth	MAN	3812.93	10.73	0.78
	truth + 10%	MAN	4298.88	12.75	0.77
	truth + 20%	MAN	4691.39	14.34	0.77
Flight #2		INS	1964.83	26.26	1.28
	truth	MAN	3503.28	10.62	0.83
	truth + 10%	MAN	4035.03	12.58	0.82
	truth + 20%	MAN	4456.09	14.12	0.81
Flight #3		INS	5761.41	25.85	1.21
	truth	MAN	2786.2	12.12	0.89
	truth + 10%	MAN	4936.7	15.17	0.87
	truth + 20%	MAN	4936.7	15.17	0.87
Flight #4		INS	5534.09	25.82	1.22
	truth	MAN	4489.31	11.25	0.82
	truth + 10%	MAN	4758.01	13.24	0.82
	truth + 20%	MAN	4990.07	14.79	0.83
Flight #5		INS	5604.81	25.79	1.24
	truth	MAN	2919.03	11.8	0.84
	truth + 10%	MAN	3940.19	13.57	0.83
	truth + 20%	MAN	5091.48	14.97	0.83

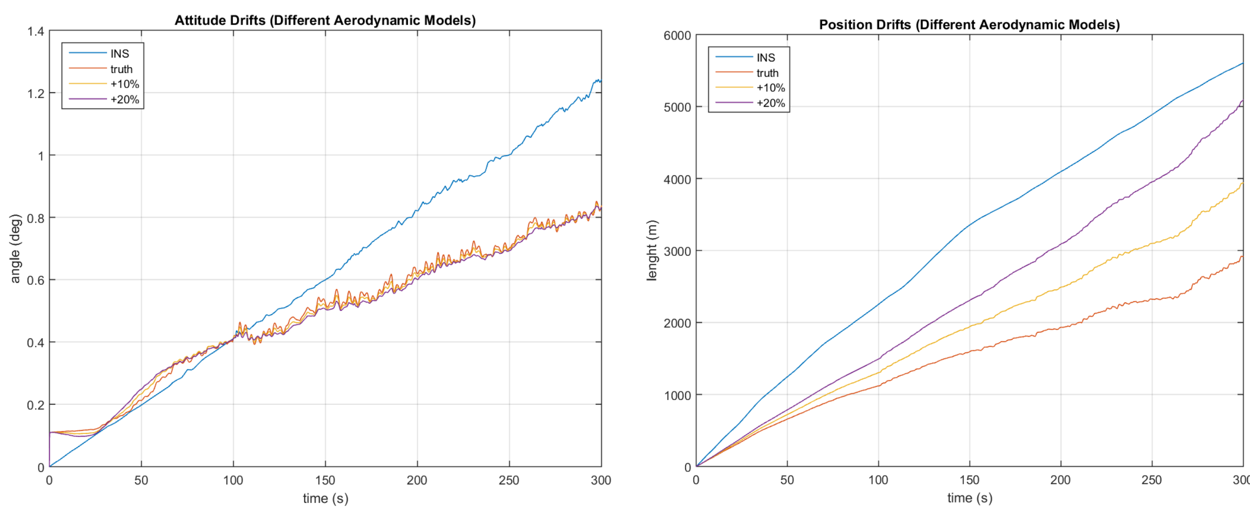

Figure 5: Position and attitude drifts related to the different aerodynamic models.

V. Conclusions

This sensitivity study confirm that considering a VDM model coupled with an UKF and combined with an INS, we obtain a higher performance navigation system. VDM-only position, velocity and attitude solutions are improved, this approach lowers INS positing solution errors by one third to half over the 5 minute simulated flights. The introduction of an airspeed sensor gives benefits in terms of velocity estimation as the introduction of an altimeter does with position estimation (z-axis component in particular of course). The scaled aerodynamic model influences the position more than the velocity solution. As expected, the performance increases in terms of position and Attitude estimation using a better IMU, however when used MAN, the impact is apparent for positioning. Future developments will involved the introduction in the model of winds, gusts and turbulence. A study about how different maneuver sequences and flight conditions affect the results of the proposed approach can be performed.

References

[1]Koifman, M. and Bar-Itzhack, I. Y., "Inertial Navigation System Aided by Aircraft Dynamics," *IEEE Transactions on Control Systems Technology*, Vol. 7, No. 4, 1999.

[2]Crocoll, P., Grcke, L., Lorenz, G. F. T., and Holzapfel, F., "Unified Model Technique for Inertial Navigation Aided by Vehicle Dynamics Model," *Journal of Institute of Navigation*, Vol. 60, No. 3, 2013, pp. 179–193.

[3]Crocoll, P., Seibold, J., Scholz, G., and Trommer, G. F., "Model-Aided Navigation for a Quadrotor Helicopter: A Novel Navigation System and First Experimental Results," *Journal of Institute of Navigation*, Vol. 61, No. 4, 2014, pp. 253–271.

[4]Bryson, M. and Sukkarieh, S., "Vehicle Model Aided Inertial Navigation for a UAV using Low-cost Sensors," *Proceedings of the Australasian Conference on Robotics and Automation*, 2004.

[5]Khagani, M. and Skaloud, J., "Autonomous Vehicle Dynamic Model-Based Navigation for Small UAVs," *Journal of Institute of Navigation*, Vol. 63, No. 3, 2016, pp. 345–358.

[6]Sequeira, C., Willis, D. J., and Peraire, J., "Comparing Aerodynamic Models for Numerical Simulation of Dynamics and Control of Aircraft," *44th AIAA Aerospace Sciences Meeting and Exhibit*, AIAA, Reno, NV, 2006.

[7]MATLAB, *version 8.5.0 (R2015a)*, The MathWorks Inc., 2015.

[8]"FlightGear Flight Simulator," version 3.4.0, version 3.4.0 (2015), http://www.flightgear.org/.

[9]GPSoft, "Satellite Navigation TOOLBOX 3.0 User's Guide," 2003, http://gpsoftnav.com/.

[10]Watson, R., Sivaneri, V., and Gross, J., "Performance Characterization of Tightly-Coupled GNSS Precise Point Positioning Inertial Navigation within a Simulation Environment," *Submitted to the 2016 AIAA Guidance Navigation and Control Conference*, 2016.

[11]"HG1930 Inertial Measurement Unit," Honeywell International, Inc., https://aerospace.honeywell.com/~/media/aerospace/files/brochures/n61-1025-000-001-hg1930-bro.pdf.

[12]Stengel, R., *Flight Dynamics*, Princeton University Press, 2004.

[13]Groves, P. D., *Principles of GNSS, inertial, and multisensor integrated navigation systems*, Artech House, 2013.

[14]Wan, E. A. and van der Merwe, R., "The Unscented Kalman Filter," *Chap. 7 in "Kalman Filtering and Neural Networks""*, 2002, pp. 221–282.

[15]Simon, D., *Optimal state estimation: Kalman, H infinity, and nonlinear approaches*, John Wiley & Sons, 2006.